Available online at www.sciencedirect.com
ScienceDirect
Journal of Sound and Vibration 320 (2009) 421–437
JOURNAL OF SOUND AND VIBRATION
www.elsevier.com/locate/jsvi

3-D vibration analysis of annular sector plates using the Chebyshev–Ritz method

D. Zhou[a,*], S.H. Lo[b], Y.K. Cheung[b]

[a]College of Civil Engineering, Nanjing University of Technology, Nanjing 210009, PR China
[b]Department of Civil Engineering, The University of Hong Kong, Hong Kong, PR China

Received 25 September 2007; received in revised form 29 July 2008; accepted 2 August 2008
Handling Editor: L.G. Tham
Available online 6 September 2008

Abstract

The three-dimensional free vibration of annular sector plates with various boundary conditions is studied by means of the Chebyshev–Ritz method. The analysis is based on the three-dimensional small strain linear elasticity theory. The product of Chebyshev polynomials satisfying the necessary boundary conditions is selected as admissible functions in such a way that the governing eigenvalue equation can be conveniently derived through an optimization process by the Ritz method. The boundary functions guarantee the satisfaction of the geometric boundary conditions of the plates and the Chebyshev polynomials provide the robustness for numerical calculation. The present study provides a full vibration spectrum for the thick annular sector plates, which cannot be given by the two-dimensional (2-D) theories such as the Mindlin theory. Comprehensive numerical results with high accuracy are systematically produced, which can be used as benchmark to evaluate other numerical methods. The effect of radius ratio, thickness ratio and sector angle on natural frequencies of the plates with a sector angle from 120° to 360° is discussed in detail. The three-dimensional vibration solutions for plates with a re-entrant sector angle (larger than 180°) and shallow helicoidal shells (sector angle larger than 360°) with a small helix angle are presented for the first time.

1. Introduction

As fundamental structural elements, plates are widely used in various engineering constructions. The vibration characteristics of annular sector plates have attracted the interest of many investigators. The early study on plate vibrations is focused on the classical plate theory (CPT), which is suitable for thin plate structures. Ramakris and Kunukkas [1] provided a closed-form analytical solution for free vibration of an annular sector plate with radial edges simply supported. Mukhopadhyay [2,3] used a semi-analytical method and Thiruvenkatachari [4,5] used the integral equation technique to analyze the vibrations of annular sector plates, respectively. Kim and Dickinson [6] used one-dimensional (1-D) orthogonal polynomials and Liew and Lam [7] used two-dimensional (2-D) orthogonal polynomials as admissible functions to study the free vibration of annular sector plates by the Rayleigh–Ritz method. Ramaiah and Vijayakumar [8] studied the

*Corresponding author.
E-mail address: dingzhou57@yahoo.com (D. Zhou).

0022-460X/$ - see front matter © 2008 Elsevier Ltd. All rights reserved.
doi:10.1016/j.jsv.2008.08.001

free vibration of annular sector plates with simply supported radial edges by a combination of the Rayleigh–Ritz method and coordinate transformation. Irie et al. [9] studied the vibration of cantilevered annular sector plates with curved radial edges by a coordinate transformation. Mizusawa [10] and Mizusawa and Kajita [11] used the spline finite element and spline strip method to analyze the free vibration of annular sector plates, respectively. Swaminadham et al. [12] compared the natural frequencies of annular sector plates from the finite element method and experiments. Seok and Tiersten [13] used a variational approximation procedure to analyze the free vibration of cantilevered annular sector plates. Houmat [14] used the hierarchical finite element method to study the free vibration of annular sector plates. Sharma et al. [15,16] integrated an analytical approach with the Chebyshev polynomials technique to study the buckling and free vibration of isotropic and laminated composite sector plates based on the first-order shear deformation theory.

For moderate thickness plates, the first-order shear deformable plate theory is commonly used, which could provide a result more accurate than that from the CPT. Liew and Liu [17] used the differential quadrature method to analyze the free vibration of thick annular sector plates. Rao et al. [18] and Guruswamy and Yang [19] used the finite element method to analyze the vibrations of thick annular sector plates. Benson and Hinton [20] and Cheung and Chan [21] used the finite strip method to carry out static and dynamic analyses of thick annular sector plates. Mizusawa [22] used the finite element method to study the natural frequencies of thick annular sector plates. Xiang et al. [23] applied the Ritz method to study the free vibration of thick annular sector plates. Leissa et al. [24,25] considered the effect of stress singularities on the vibration analysis of thick annular sector plates and presented the corner functions to improve the convergence of the numerical solutions.

However, only three papers have been found in the published literature about the vibrations of annular sector plates based on the three-dimensional (3-D) elasticity theory. Mizusawa [26] used the finite prism method, Houmat [27] used the hierarchical finite element method and Liew et al. [28] used the 2-D orthogonal polynomials in the Ritz method to analyze the free vibration of thick annular sector plates. The existing results are simply too scarce for engineering applications and comparative studies, and only results for annular sector plates with sector angles not larger than 90° are available.

In the present study, the Chebyshev–Ritz method is applied to study the free vibration of thick annular sector plates. Admissible functions can be derived conveniently from a product of the Chebyshev polynomials and boundary functions in such a way that the geometric boundary conditions are implicitly satisfied. The present admissible functions show a distinct advantage over admissible functions based on simple polynomials as Chebyshev polynomials are numerically stable even when a large number of admissible functions are employed for the solutions of higher vibration modes [29,30].

2. Basic formulation

Consider an annular sector plate shown in Fig. 1. The plate is of constant thickness h, inner radius R_0, outer radius R_1 and sector angle θ_0. A cylindrical coordinate system (r, θ, z) is taken to describe the displacement components u, v, w at a generic point in the radial, circumferential and thickness directions. The linear elastic strain energy P of the plate can be written in the integral form

$$P = \frac{E}{2(1+v)} \int_{R_0}^{R_1} \int_0^{\theta_0} \int_{-h/2}^{h/2} \left[\frac{v}{1-2v} (\varepsilon_{rr} + \varepsilon_{\theta\theta} + \varepsilon_{zz})^2 + \varepsilon_{rr}^2 + \varepsilon_{\theta\theta}^2 + \varepsilon_{zz}^2 + \frac{1}{2}(\varepsilon_{r\theta}^2 + \varepsilon_{rz}^2 + \varepsilon_{\theta z}^2) \right] r \, dz \, d\theta \, dr \tag{1}$$

where E is Young's modulus and v is Poisson's ratio. The strain components ε_{ij} $(i, j = r, \theta, z)$ are defined as follows:

$$\varepsilon_{rr} = \frac{\partial u}{\partial r}, \quad \varepsilon_{\theta\theta} = \frac{u}{r} + \frac{\partial v}{r \partial \theta}, \quad \varepsilon_{zz} = \frac{\partial w}{\partial z}, \quad \varepsilon_{r\theta} = \frac{\partial u}{r \partial \theta} + \frac{\partial v}{\partial r} - \frac{v}{r}, \quad \varepsilon_{rz} = \frac{\partial u}{\partial z} + \frac{\partial w}{\partial r}, \quad \varepsilon_{\theta z} = \frac{\partial v}{\partial z} + \frac{\partial w}{r \partial \theta} \tag{2}$$

The kinetic energy T of the plate is given by

$$T = \frac{\rho}{2} \int_{R_0}^{R_1} \int_0^{\theta_0} \int_{-h/2}^{h/2} \left(\left(\frac{\partial u}{\partial t} \right)^2 + \left(\frac{\partial v}{\partial t} \right)^2 + \left(\frac{\partial w}{\partial t} \right)^2 \right) r \, dz \, d\theta \, dr \tag{3}$$

where ρ is the mass density per unit volume.

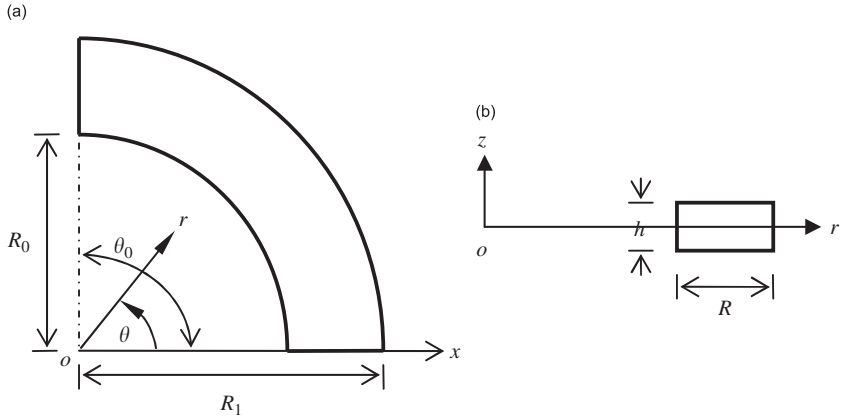

Fig. 1. A sector plate: (a) the plan and (b) the cross-section.

For simplicity and convenience in mathematical formulation, the following dimensionless parameters are introduced:

$$\bar{r} = \frac{2r}{R} - \psi, \quad \bar{\theta} = \frac{2\theta}{\theta_0} - 1, \quad \bar{z} = \frac{2z}{h} \tag{4}$$

where $R = R_1 - R_0$ is the width of the plate in the radial direction and $\psi = (R_1 + R_0)/(R_1 - R_0)$.

For the free vibration analysis, the displacement components of the plate can be expressed into the product of displacement amplitude functions about coordinates $\bar{r}, \bar{\theta}, \bar{z}$ and an exponent function about time t as follows:

$$u(r,\theta,z,t) = U(\bar{r},\bar{\theta},\bar{z})e^{i\omega t}, \quad v(r,\theta,z,t) = V(\bar{r},\bar{\theta},\bar{z})e^{i\omega t}, \quad w(r,\theta,z,t) = W(\bar{r},\bar{\theta},\bar{z})e^{i\omega t} \tag{5}$$

where ω denotes the natural frequency of the plate and $i = \sqrt{-1}$. Substituting Eqs. (2), (4) and (5) into Eqs. (1) and (3), the maximum potential energy $P_{\max}$ and the maximum kinetic energy $T_{\max}$ can be written as

$$\begin{aligned}
P_{\max} = {} & \frac{Eh\theta_0}{16(1+\nu)} \int_{-1}^{1}\int_{-1}^{1}\int_{-1}^{1} \left(\frac{2(1-\nu)}{1-2\nu} \left[\left(\frac{\partial U}{\partial \bar{r}} \right)^2 + \frac{U^2}{(\bar{r}+\psi)^2} \right] + \frac{4\nu}{1-2\nu} \frac{U}{\bar{r}+\psi} \frac{\partial U}{\partial \bar{r}} + \frac{4}{\theta_0^2(\bar{r}+\psi)^2} \left(\frac{\partial U}{\partial \bar{\theta}} \right)^2 \right. \\
& + \frac{1}{\gamma^2} \left(\frac{\partial U}{\partial \bar{z}} \right)^2 + \frac{8(1-\nu)}{1-2\nu} \frac{U}{\theta_0(\bar{r}+\psi)^2} \frac{\partial V}{\partial \bar{\theta}} + \frac{8\nu}{(1-2\nu)\theta_0} \frac{1}{(\bar{r}+\psi)} \frac{\partial U}{\partial \bar{r}} \frac{\partial V}{\partial \bar{\theta}} + \frac{4}{\theta_0(\bar{r}+\psi)} \frac{\partial U}{\partial \bar{\theta}} \frac{\partial V}{\partial \bar{r}} \\
& - \frac{4}{\theta_0(\bar{r}+\psi)^2} \frac{\partial U}{\partial \bar{\theta}} V + \frac{4\nu}{(1-2\nu)\gamma} \left[\frac{\partial U}{\partial \bar{r}} \frac{\partial W}{\partial \bar{z}} + \frac{U}{\bar{r}+\psi} \frac{\partial W}{\partial \bar{z}} \right] + \frac{2}{\gamma} \frac{\partial U}{\partial \bar{z}} \frac{\partial W}{\partial \bar{r}} \\
& + \frac{8(1-\nu)}{(1-2\nu)\theta_0^2} \frac{1}{(\bar{r}+\psi)^2} \left(\frac{\partial V}{\partial \bar{\theta}} \right)^2 + \left(\frac{\partial V}{\partial \bar{r}} \right)^2 + \frac{V^2}{(\bar{r}+\psi)^2} + \frac{1}{\gamma^2} \left(\frac{\partial V}{\partial \bar{z}} \right)^2 - \frac{2}{\bar{r}+\psi} V \frac{\partial V}{\partial \bar{r}} \\
& + \frac{8\nu}{(1-2\nu)\theta_0\gamma} \frac{1}{\bar{r}+\psi} \frac{\partial V}{\partial \bar{\theta}} \frac{\partial W}{\partial \bar{z}} + \frac{4}{\theta_0\gamma(\bar{r}+\psi)} \frac{\partial V}{\partial \bar{z}} \frac{\partial W}{\partial \bar{\theta}} \\
& \left. + \frac{2(1-\nu)}{\gamma^2(1-2\nu)} \left(\frac{\partial W}{\partial \bar{z}} \right)^2 + \left(\frac{\partial W}{\partial \bar{r}} \right)^2 + \frac{4}{\theta_0^2(\bar{r}+\psi)^2} \left(\frac{\partial W}{\partial \bar{\theta}} \right)^2 \right) (\bar{r}+\psi)\, d\bar{r}\, d\bar{\theta}\, d\bar{z} \\
T_{\max} = {} & \frac{\rho h \theta_0 R^2}{32} \omega^2 \int_{-1}^{1}\int_{-1}^{1}\int_{-1}^{1} \left((U)^2 + (V)^2 + (W)^2 \right) (\bar{r}+\psi)\, d\bar{r}\, d\bar{\theta}\, d\bar{z}
\end{aligned} \tag{6}$$

where $\gamma = h/R$. Each of the displacement amplitude functions takes the form of a triplicate series of Chebyshev polynomials suitably combined with boundary functions as follows:

$$U(\bar{r},\bar{\theta},\bar{z}) = F_{ur}(\bar{r})F_{u\theta}(\bar{\theta})\sum_{i=1}^{\infty}\sum_{j=1}^{\infty}\sum_{k=1}^{\infty}A_{ijk}G_i(\bar{r})G_j(\bar{\theta})G_k(\bar{z})$$

$$V(\bar{r},\bar{\theta},\bar{z}) = F_{vr}(\bar{r})F_{v\theta}(\bar{\theta})\sum_{l=1}^{\infty}\sum_{m=1}^{\infty}\sum_{n=1}^{\infty}B_{lmn}G_l(\bar{r})G_m(\bar{\theta})G_n(\bar{z})$$

$$W(\bar{r},\bar{\theta},\bar{z}) = F_{wr}(\bar{r})F_{w\theta}(\bar{\theta})\sum_{p=1}^{\infty}\sum_{q=1}^{\infty}\sum_{r=1}^{\infty}C_{pqr}G_p(\bar{r})G_q(\bar{\theta})G_r(\bar{z}) \tag{7}$$

where A_{ijk}, B_{lmn} and C_{pqr} are the coefficients yet to be determined. $G_s(\chi)$ ($s = i, j, k, l, m, n, p, q, r$, $\chi = \bar{r}, \bar{\theta}, \bar{z}$) are the Chebyshev polynomial series, which are given by

$$G_s(\chi) = \cos[(s-1)\arccos(\chi)], \quad s = 1, 2, 3, \ldots \tag{8}$$

$F_{ur}(\bar{r})$, $F_{vr}(\bar{r})$ and $F_{wr}(\bar{r})$ are the boundary functions of displacements u, v and w in the r direction, respectively. $F_{u\theta}(\bar{\theta})$, $F_{v\theta}(\bar{\theta})$ and $F_{w\theta}(\bar{\theta})$ are those of displacements u, v and w in the θ direction, respectively. The boundary functions can be written as follows:

$$F_{\alpha r}(\bar{r}) = F^0_{\alpha r}(\bar{r})F^1_{\alpha r}(\bar{r}), \quad F_{\alpha\theta} = F^0_{\alpha\theta}(\bar{\theta})F^1_{\alpha\theta}(\bar{\theta}), \quad \alpha = u, v, w \tag{9}$$

where $F^0_{\alpha r}(\bar{r})$ and $F^1_{\alpha\theta}(\bar{r})$ are the boundary functions at $r = R_0$ and $r = R_1$, respectively. $F^0_{\alpha\theta}(\bar{\theta})$ and $F^1_{\alpha\theta}(\bar{\theta})$ are those at $\theta = 0$ and $\theta = \theta_0$, respectively. The boundary functions corresponding to common boundary conditions are given in Table 1. The energy functional of the plate is defined as

$$\Pi = P_{\max} - T_{\max} \tag{10}$$

Substituting Eq. (7) into Eq. (6), then minimizing energy functional (10), i.e.

$$\frac{\partial\Pi}{\partial A_{ijk}} = 0, \quad \frac{\partial\Pi}{\partial B_{lmn}} = 0, \quad \frac{\partial\Pi}{\partial C_{pqr}} = 0 \tag{11}$$

Table 1
Boundary functions (BF) for various common boundary conditions

BF	Clamped	Free	Sliding	Hard simply supported	Soft simply supported
$F^0_{ur}(\bar{r})$	$\bar{r}+1$	1	$\bar{r}+1$	1	1
$F^0_{vr}(\bar{r})$	$\bar{r}+1$	1	1	$\bar{r}+1$	1
$F^0_{wr}(\bar{r})$	$\bar{r}+1$	1	1	$\bar{r}+1$	$\bar{r}+1$
$F^1_{ur}(\bar{r})$	$\bar{r}-1$	1	$\bar{r}-1$	1	1
$F^1_{vr}(\bar{r})$	$\bar{r}-1$	1	1	$\bar{r}-1$	1
$F^1_{wr}(\bar{r})$	$\bar{r}-1$	1	1	$\bar{r}-1$	$\bar{r}-1$
$F^0_{u\theta}(\bar{\theta})$	$\bar{\theta}+1$	1	$\bar{\theta}+1$	1	1
$F^0_{v\theta}(\bar{\theta})$	$\bar{\theta}+1$	1	1	$\bar{\theta}+1$	1
$F^0_{w\theta}(\bar{\theta})$	$\bar{\theta}+1$	1	1	$\bar{\theta}+1$	$\bar{\theta}+1$
$F^1_{u\theta}(\bar{\theta})$	$\bar{\theta}-1$	1	$\bar{\theta}-1$	1	1
$F^1_{v\theta}(\bar{\theta})$	$\bar{\theta}-1$	1	1	$\bar{\theta}-1$	1
$F^1_{w\theta}(\bar{\theta})$	$\bar{\theta}-1$	1	1	$\bar{\theta}-1$	$\bar{\theta}-1$

Note: hard simply supported means the zero displacement conditions in both the z direction and the tangential direction along the edge, while soft simply supported means the zero displacement condition only in the z direction.

and truncating i, j, k up to $I+1$, $J+1$ and $K+1$, respectively, one has the following eigenvalue equation:

$$\left(\begin{bmatrix} [K_{uu}] & [K_{uv}] & [K_{uw}] \\ [K_{uv}]^{\mathrm{T}} & [K_{vv}] & [K_{vw}] \\ [K_{uw}]^{\mathrm{T}} & [K_{vw}]^{\mathrm{T}} & [K_{ww}] \end{bmatrix} - \Omega^2 \begin{bmatrix} [M_{uu}] & 0 & 0 \\ 0 & [M_{vv}] & 0 \\ 0 & 0 & [M_{ww}] \end{bmatrix} \right) \begin{Bmatrix} \{A\} \\ \{B\} \\ \{C\} \end{Bmatrix} = \begin{Bmatrix} \{0\} \\ \{0\} \\ \{0\} \end{Bmatrix} \tag{12}$$

in which, $\Omega = \omega R\sqrt{\rho/E}$, $[K_{ij}]$ and $[M_{ij}]$ $(i, j = u, v, w)$ are the stiffness sub-matrices and the diagonal mass sub-matrices, respectively. The column vectors $\{A\}$, $\{B\}$ and $\{C\}$ are composed of the unknown coefficients as follows:

$$\{A\} = \begin{Bmatrix} A_{111} \\ A_{112} \\ \vdots \\ A_{11K} \\ A_{121} \\ \vdots \\ A_{12K} \\ \vdots \\ A_{1JK} \\ \vdots \\ A_{IJK} \end{Bmatrix}, \quad \{B\} = \begin{Bmatrix} B_{111} \\ B_{112} \\ \vdots \\ B_{11N} \\ B_{121} \\ \vdots \\ B_{12N} \\ \vdots \\ B_{1MN} \\ \vdots \\ A_{LMN} \end{Bmatrix}, \quad \{C\} = \begin{Bmatrix} C_{111} \\ C_{112} \\ \vdots \\ C_{11R} \\ C_{121} \\ \vdots \\ C_{12R} \\ \vdots \\ C_{1QR} \\ \vdots \\ C_{PQR} \end{Bmatrix} \tag{13}$$

The elements in the sub-matrices $[K_{ij}]$ and $[M_{ij}]$ $(i, j = u, v, w)$ are given by

$$\begin{aligned}
[K_{uu}] &= \frac{2(1-v)}{1-2v} D^{1,1,1}_{uiu\bar{i}} Q^{0,0}_{uju\bar{j}} H^{0,0}_{uku\bar{k}} + D^{1,1,-1}_{uiu\bar{i}} Q^{0,0}_{uju\bar{j}} H^{0,0}_{uku\bar{k}} + \frac{2v}{1-2v}(D^{0,1,0}_{uiu\bar{i}} + D^{1,0,0}_{uiu\bar{i}}) Q^{0,0}_{uju\bar{j}} H^{0,0}_{uku\bar{k}} \\
&\quad + \frac{4}{\theta_0^2} D^{1,1,-1}_{uiu\bar{i}} Q^{1,1}_{uju\bar{j}} H^{0,0}_{uku\bar{k}} + \frac{1}{\gamma} D^{0,0,1}_{uiu\bar{i}} Q^{0,0}_{uju\bar{j}} H^{1,1}_{uku\bar{k}} \\
[K_{uw}] &= \frac{4(1-v)}{(1-2v)\theta_0} D^{0,0,-1}_{uiv\bar{i}} Q^{0,0}_{ujv\bar{n}} H^{0,0}_{ukv\bar{n}} + \frac{4v}{(1-2v)\theta_0} D^{0,0,-1}_{uiv\bar{i}} Q^{0,1}_{ujv\bar{n}} H^{0,0}_{ukv\bar{n}} \\
&\quad + \frac{2}{\theta_0}(D^{0,1,0}_{uiv\bar{i}} - D^{0,0,-1}_{uiv\bar{i}}) Q^{0,1}_{ujv\bar{n}} H^{0,0}_{ukv\bar{n}} \\
[K_{uw}] &= \frac{2v}{(1-2v)\gamma} \left(\frac{2}{\theta_0}(D^{1,0,1}_{uiw\bar{p}} + D^{0,0,0}_{uiw\bar{p}}) Q^{0,0}_{ujw\bar{q}} H^{0,1}_{ukw\bar{r}} \right) + \frac{1}{\gamma} D^{0,1,1}_{uiw\bar{p}} Q^{0,0}_{ujw\bar{q}} H^{1,0}_{ukw\bar{r}} \\
[K_{vv}] &= \frac{8(1-v)}{(1-2v)\theta_0^2} D^{0,0,-1}_{vlv\bar{l}} Q^{1,1}_{vmv\bar{n}} H^{0,0}_{vnv\bar{n}} + D^{1,1,1}_{vlv\bar{l}} Q^{0,0}_{vmv\bar{n}} H^{0,0}_{vnv\bar{n}} + D^{0,0,1}_{vlv\bar{l}} Q^{0,0}_{vmv\bar{n}} H^{0,0}_{vnv\bar{n}} \\
&\quad + \frac{1}{\gamma^2} D^{0,0,1}_{vlv\bar{l}} Q^{0,0}_{vmv\bar{n}} H^{1,1}_{vnv\bar{n}} - (D^{0,1,0}_{vlv\bar{l}} + D^{1,0,0}_{vlv\bar{l}}) Q^{0,0}_{vmv\bar{n}} H^{0,0}_{vnv\bar{n}} \\
[K_{vw}] &= \frac{4v}{(1-2v)\theta_0\gamma} D^{0,0,0}_{vlw\bar{p}} Q^{1,0}_{vmw\bar{q}} H^{0,1}_{vnw\bar{r}} + \frac{2}{\theta_0\gamma} D^{0,0,0}_{vlw\bar{p}} Q^{0,1}_{vmw\bar{q}} H^{1,0}_{vnw\bar{r}} \\
[K_{ww}] &= \frac{2(1-v)}{(1-2v)\gamma^2} D^{0,0,1}_{wpw\bar{p}} Q^{0,0}_{wqw\bar{q}} H^{1,1}_{wrw\bar{r}} + D^{1,1,1}_{wpw\bar{p}} Q^{0,0}_{wqw\bar{q}} H^{0,0}_{wrw\bar{r}} + \frac{4}{\theta_0^2} D^{0,0,-1}_{wpw\bar{p}} Q^{1,1}_{wqw\bar{q}} H^{0,0}_{wrw\bar{r}} \\
[M_{uu}] &= D^{0,0,1}_{uiu\bar{i}} G^{0,0}_{uju\bar{j}} H^{0,0}_{uku\bar{k}}/2(1+v), \quad [M_{vv}] = D^{0,0,1}_{vlv\bar{l}} G^{0,0}_{vmv\bar{n}} H^{0,0}_{vnv\bar{n}}/2(1+v) \\
[M_{ww}] &= D^{0,0,1}_{wpw\bar{p}} G^{0,0}_{wqw\bar{q}} H^{0,0}_{wrw\bar{r}}/2(1+v)
\end{aligned} \tag{14}$$

Table 2
Convergence of λ for cantilevered annular sector plates clamped on one straight edge and having $\theta_0 = 120^\circ$, $R_0/R_1 = 0.5$

h/R	$I \times J \times K$	λ_1	λ_2	λ_3	λ_4	λ_5	λ_6
Antisymmetric modes in thickness direction							
0.01	$18 \times 18 \times 1$	1.7956	5.9855	13.661	20.624	36.233	40.314
	$18 \times 18 \times 2$	1.6964	5.7464	13.247	19.654	34.905	38.399
	$18 \times 18 \times 3$	1.6964	5.7464	13.247	19.654	34.905	38.399
	$22 \times 22 \times 2$	1.6959	5.7431	13.240	19.646	34.888	38.381
	$26 \times 26 \times 2$	1.6955	5.7413	13.237	19.642	34.880	38.371
	$30 \times 30 \times 2$	1.6948	5.7402	13.235	19.639	34.876	38.365
0.2	$16 \times 16 \times 2$	1.6570	5.4593	12.141	18.612	31.405	34.952
	$16 \times 16 \times 3$	1.6568	5.4588	12.139	18.611	31.398	34.947
	$16 \times 16 \times 4$	1.6568	5.4588	12.139	18.611	31.398	34.947
	$20 \times 20 \times 3$	1.6565	5.4573	12.138	18.606	31.394	34.939
	$22 \times 22 \times 3$	1.6564	5.4570	12.137	18.605	31.393	34.937
	$24 \times 24 \times 3$	1.6564	5.4567	12.137	18.604	31.393	34.936
0.5	$14 \times 14 \times 3$	1.5354	4.7865	9.7465	15.619	23.314	26.885
	$14 \times 14 \times 4$	1.5353	4.7863	9.7458	15.618	23.312	26.884
	$14 \times 14 \times 5$	1.5353	4.7863	9.7458	15.618	23.312	26.884
	$16 \times 16 \times 4$	1.5351	4.7856	9.7451	15.616	23.311	26.881
	$18 \times 18 \times 4$	1.5350	4.7851	9.7447	15.615	23.310	26.880
	$20 \times 20 \times 4$	1.5350	4.7848	9.7445	15.614	23.310	26.879
Symmetric modes in thickness direction							
0.2	$16 \times 16 \times 3$	6.8828	21.590	43.963	69.248	90.479	104.65
	$16 \times 16 \times 4$	6.8828	21.590	43.963	69.248	90.479	104.65
	$20 \times 20 \times 3$	6.8817	21.587	43.960	69.243	90.472	104.65
	$22 \times 22 \times 3$	6.8814	21.586	43.959	69.242	90.470	104.65
	$24 \times 24 \times 3$	6.8812	21.585	43.959	69.241	90.469	104.65
0.5	$14 \times 14 \times 4$	2.7611	8.6477	17.609	27.726	36.195	41.855
	$14 \times 14 \times 5$	2.7611	8.6477	17.609	27.726	36.195	41.855
	$16 \times 16 \times 4$	2.7607	8.6467	17.608	27.724	36.193	41.854
	$18 \times 18 \times 4$	2.7605	8.6460	17.608	27.723	36.191	41.853
	$20 \times 20 \times 4$	2.7604	8.6456	17.607	27.723	36.190	41.853

in which

$$
\begin{aligned}
D^{a,b,c}_{\alpha\sigma\beta\bar{\sigma}} &= \int_{-1}^{1} \frac{d^a[F_{\alpha r}(\bar{r})P_{\sigma}(\bar{r})]}{\mathrm{d}\bar{r}^a} \frac{d^b[F_{\beta r}(\bar{r})P_{\bar{\sigma}}(\bar{r})]}{\mathrm{d}\bar{r}^b}(\bar{r}+\psi)^c \,\mathrm{d}\bar{r} \\
Q^{a,b}_{\alpha\xi\beta\bar{\xi}} &= \int_{-1}^{1} \frac{d^a[F_{\alpha\theta}(\bar{\theta})P_{\xi}(\bar{\theta})]}{\mathrm{d}\bar{\theta}^a} \frac{d^b[F_{\beta\theta}(\bar{\theta})P_{\bar{\xi}}(\bar{\theta})]}{\mathrm{d}\bar{\theta}^b} \,\mathrm{d}\bar{\theta} \\
H^{a,b}_{\alpha\tau\beta\bar{\tau}} &= \int_{-1}^{1} \frac{d^a P_{\tau}(\bar{z})}{\mathrm{d}\bar{z}^a} \frac{d^b P_{\bar{\tau}}(\bar{z})}{\mathrm{d}\bar{z}^b} \,\mathrm{d}\bar{z} \\
& a;b = 0;1, \quad c = 0;1;-1, \quad \alpha;\beta = u;v;w, \quad \sigma = i;l;p, \quad \bar{\sigma} = \bar{i};\bar{l};\bar{p}, \quad \xi = j;m;q \\
& \bar{\xi} = \bar{j};\bar{m};\bar{q}, \quad \tau = k;n;r, \quad \bar{\tau} = \bar{k};\bar{n};\bar{r}
\end{aligned} \tag{15}
$$

In the numerical computations, the piece-wise Gaussian quadrature is used to evaluate the integrals in Eq. (15).

3. Convergence and comparative studies

In the following analysis, Poisson's ratio is fixed at $v = 0.3$ and all the simple supports mean hard simple supports unless stated otherwise. To be consistent with the frequency parameters defined in the literature, two

Table 3
Convergence of λ for annular sector plates clamped on one straight edge and having $\theta_0 = 240^\circ$, $R_0/R_1 = 0.5$

h/R	$I \times J \times K$	λ_1	λ_2	λ_3	λ_4	λ_5	λ_6
Antisymmetric modes in the thickness direction							
0.01	$18 \times 18 \times 1$	1.8647	4.5829	9.4245	15.656	15.869	23.787
	$18 \times 18 \times 2$	1.7545	4.3298	8.9672	15.007	15.147	22.737
	$18 \times 18 \times 3$	1.7545	4.3298	8.9672	15.007	15.147	22.737
	$22 \times 22 \times 2$	1.7533	4.3265	8.9599	14.999	15.136	22.720
	$26 \times 26 \times 2$	1.7527	4.3246	8.9558	14.995	15.130	22.710
	$30 \times 30 \times 2$	1.7522	4.3236	8.9533	14.993	15.126	22.704
0.2	$16 \times 16 \times 2$	1.7251	4.2281	8.6710	13.786	14.478	21.444
	$16 \times 16 \times 3$	1.7251	4.2279	8.6707	13.785	14.478	21.443
	$16 \times 16 \times 4$	1.7251	4.2279	8.6707	13.785	14.478	21.443
	$20 \times 20 \times 3$	1.7241	4.2251	8.6646	13.783	14.469	21.429
	$22 \times 22 \times 3$	1.7238	4.2243	8.6629	13.782	14.466	21.426
	$24 \times 24 \times 3$	1.7237	4.2238	8.6618	13.782	14.465	21.423
0.5	$14 \times 14 \times 3$	1.6310	3.9289	7.7558	12.427	11.126	17.398
	$14 \times 14 \times 4$	1.6309	3.9289	7.7557	12.427	11.126	17.397
	$14 \times 14 \times 5$	1.6309	3.9288	7.7557	12.427	11.126	17.397
	$16 \times 16 \times 4$	1.6304	3.9272	7.7527	12.423	11.125	17.396
	$18 \times 18 \times 4$	1.6301	3.9262	7.7507	12.420	11.125	17.395
	$20 \times 20 \times 4$	1.6299	3.9255	7.7495	12.419	11.125	17.394
Symmetric modes in the thickness direction							
0.2	$16 \times 16 \times 3$	12.453	24.577	39.701	46.012	59.570	65.291
	$16 \times 16 \times 4$	12.453	24.577	39.701	46.012	59.570	65.291
	$20 \times 20 \times 3$	12.446	24.570	39.693	46.006	59.559	65.279
	$22 \times 22 \times 3$	12.444	24.568	39.691	46.005	59.557	65.275
	$24 \times 24 \times 3$	12.443	24.567	39.689	46.004	59.555	65.273
0.5	$14 \times 14 \times 4$	4.9956	9.8412	15.899	18.430	23.863	26.125
	$14 \times 14 \times 5$	4.9956	9.8412	15.899	18.430	23.863	26.125
	$16 \times 16 \times 4$	4.9937	9.8392	15.896	18.428	23.860	26.122
	$18 \times 18 \times 4$	4.9924	9.8379	15.895	18.427	23.858	26.120
	$20 \times 20 \times 4$	4.9915	9.8371	15.894	18.426	23.857	26.118

non-dimensional eigenvalues are used: $\lambda = \omega R_1^2 \sqrt{\rho h/D}$ and $\bar{\Omega} = \omega R_1 \sqrt{\rho/E}$. For plates, the vibration modes can always be divided into antisymmetric and symmetric ones in the thickness direction. In this case, the computational cost can be reduced by taking $k,n = 2,4,6,\ldots$, $r = 1,3,5,\ldots$ for the antisymmetric vibration in the thickness direction and $k,n = 1,3,5,\ldots$, $r = 2,4,6,\ldots$ for the symmetric vibration in the thickness direction, respectively.

The convergence studies of the frequency parameter λ for cantilevered annular sector plates clamped at a straight edge are carried out to study the convergence characteristics of the present method as shown in Table 2. The radius ratio of the plates is $R_0/R_1 = 0.5$ and the sector angle is $\theta_0 = 120^\circ$. Three different thickness ratios $h/R = 0.01,0.2,0.5$ are examined, which correspond to thin, moderately thick and thick plates, respectively. For simplicity, equal numbers of terms of admissible functions are taken in displacement amplitude functions U, V and W although different numbers of terms among U, V and W might provide a more rapid convergence. It is seen in Table 2 that the convergent rate of λ is consistent with the upper-bound characteristics of the Ritz method. Namely, as the number of terms of the admissible functions increases, frequency parameter λ tends to converge monotonically from the above. With the increase in plate thickness, the number of terms needed in the z direction should be increased and at the same time the number of terms used in the x and y directions can be reduced.

Table 3 gives the convergence of the cantilevered annular sector plates clamped at a straight edge with $R_0/R_1 = 0.5$ and $\theta_0 = 240^\circ$. It is obvious that in such a case, the sector angle is re-entrant. It is seen that the

Table 4
Comparison of λ/π^2 for annular sector plates with various boundary conditions for $R_0/R_1 = 0.4$ and $\theta_0 = 90^\circ$

h/R	BC	Sources	λ_1/π^2	λ_2/π^2	λ_3/π^2	λ_4/π^2	λ_5/π^2	λ_6/π^2
1/6	SSSS	Ref. [28]	3.4476	5.5699	6.0808	8.6811	9.9621	10.248
		Present	3.4476	5.5699	6.0807	8.6811	9.9620	10.248
	SSFF	Ref. [28]	2.6606	3.1100	3.2111	4.8673	5.8231	7.4718
		Present	2.6602	3.1058	3.2107	4.8665	5.8203	7.4713
	CCFF	Ref. [28]	5.2651	5.5023	6.5224	8.6305	10.590	11.735
		Present	5.2615	5.4983	6.5172	8.6262	10.584	11.728
	CCSS	Ref. [28]	5.6650	7.1019	9.8012	11.195	13.007	13.307
		Present	5.6625	7.0999	9.7982	11.194	13.002	13.304
	CCCC	Ref. [28]	5.9306	7.8931	10.918	13.141	14.490	14.565
		Present	5.9274	7.8885	10.910	13.135	14.480	14.563
1/3	SSSS	Ref. [28]	2.9973	3.0424	4.5870	4.9818	5.5973	6.7040
		Present	2.9973	3.0424	4.5870	4.9818	5.5973	6.7040
	SSFF	Ref. [28]	1.5608	2.3558	2.7829	2.9136	4.0289	4.6820
		Present	1.5587	2.3556	2.7827	2.9121	4.0288	4.6812
	CCFF	Ref. [28]	3.8839	4.0336	4.7411	5.2979	6.2429	6.7281
		Present	3.8821	4.0318	4.7494	5.2949	6.2415	6.7243
	CCSS	Ref. [28]	4.1722	5.2634	5.5973	7.0733	7.1145	8.4995
		Present	4.1710	5.2625	5.5973	7.0730	7.1136	8.4976
	CCCC	Ref. [28]	4.3755	5.6945	7.2911	7.5643	8.5621	9.4678
		Present	4.3738	5.5926	7.2904	7.5617	8.5600	9.4663

Note: BC means boundary conditions, the first two letters mean the boundary conditions at the straight edges and the other two letters mean those at the curved edges, in which S = simply supported, C = clamped and F = free.

Table 5
Comparison of $\bar{\Omega} = \omega R_1\sqrt{\rho/E}$ for flexural vibration of annular sector plates simply supported on two straight edges and free on other edges for $R_0/R_1 = 0.5$

h/R	θ_0 (deg)	Methods	$\bar{\Omega}_1$	$\bar{\Omega}_2$	$\bar{\Omega}_3$	$\bar{\Omega}_4$	$\bar{\Omega}_5$
0.01	30	HFEM [26]	0.071	0.175	0.266	0.305	0.496
		Present	0.071	0.175	0.266	0.305	0.496
	60	HFEM [26]	0.017	0.071	0.072	0.154	0.175
		Present	0.017	0.071	0.072	0.154	0.175
0.2	30	HFEM [26]	1.304	2.929	4.180	4.617	6.883
		Present	1.304	2.929	4.180	4.617	6.883
	60	HFEM [26]	0.335	1.286	1.304	2.626	2.929
		Present	0.335	1.286	1.304	2.626	2.929
0.6	30	HFEM [26]	2.750	5.024	6.494	6.656	6.868
		Present	2.750	5.024	6.494	6.656	6.868
	60	HFEM [26]	0.863	2.565	2.750	4.715	5.024
		Present	0.863	2.565	2.750	4.715	5.024
1.0	30	HFEM [26]	3.309	3.897	5.142	5.748	6.333
		Present	3.309	3.897	5.142	5.748	6.333
	60	HFEM [26]	1.175	2.792	3.309	3.897	4.933
		Present	1.175	2.792	3.309	3.897	4.933

Note: HFEM means hierarchical finite element method.

convergence pattern of data in Table 3 is similar to that in Table 2. Comparing Tables 2 and 3, we can see that using the same number of terms, the convergence rate for the plates with the sector angle $\theta_0 = 120^\circ$ is more rapid than that for the plates with the sector angle $\theta_0 = 240^\circ$. This phenomenon can be attributed

Table 6
Comparison of fundamental frequency parameter $\lambda = \omega R_1^2\sqrt{\rho h/D}$ for flexural vibration of annular sector plates with two straight edges simply supported for $R_0/R_1 = 0.5$

θ_0 (deg)	h/R	Theories	F–F	S–S	C–C	F–C	F–S
195	0.01	Classical [25]	0.1850	41.5375	90.0837	21.4263	10.8761
		3-D	0.1856	41.5301	90.1125	21.4074	10.8522
	0.2	Mindlin [25]	0.1784	38.6356	70.8090	19.9986	10.2268
		3-D	0.1785	38.7635	71.9146	20.0967	10.2386
	0.4	Mindlin [25]	0.1706	32.8713	48.6618	17.5822	9.3661
		3-D	0.1707	33.1895	50.0059	17.7636	9.3961
210	0.01	Classical [25]	0.3239	41.3313	89.9678	20.9496	10.2631
		3-D	0.3233	41.3242	90.0265	20.9368	10.2418
	0.2	Mindlin [25]	0.3113	38.4554	70.7344	19.6097	9.6643
		3-D	0.3114	38.5820	71.8406	19.7064	9.6751
	0.4	Mindlin [25]	0.2968	32.7340	48.6117	17.2943	8.8769
		3-D	0.2971	33.0498	49.9566	17.4733	8.9043
270	0.01	Classical [25]	0.6116	40.8220	89.6828	19.7282	8.5788
		3-D	0.6104	40.8152	89.7655	19.7258	8.5635
	0.2	Mindlin [25]	0.5812	38.0095	70.5516	18.6218	8.1304
		3-D	0.5815	38.1335	71.6588	18.7149	8.1386
	0.4	Mindlin [25]	0.5481	32.3938	48.4901	16.5657	7.5461
		3-D	0.5488	32.7038	49.8361	16.7386	7.5670
360	0.01	Classical [25]	0.7044	40.4811	89.4931	18.8711	7.2502
		3-D	0.7029	40.4748	89.6519	18.8831	7.2418
	0.2	Mindlin [25]	0.6613	37.7107	70.4307	17.9366	6.9363
		3-D	0.6608	37.8329	71.5435	18.0283	6.9426
	0.4	Mindlin [25]	0.6151	32.1654	48.4105	16.0630	6.5171
		3-D	0.6161	32.4715	49.7559	16.2316	6.5332

Note: classical means classical thin plate theory and Mindlin means Mindlin moderately thick plate theory.

Table 7
Comparison of $\lambda = \omega R_1^2\sqrt{\rho h/D}$ for sector plates fixed at four edges with $R_0/R_1 = 0.5$, $h/R = 0.4$

θ_0 (deg)	Methods	λ_1	λ_2	λ_3	λ_4	λ_5	λ_6
30	Mindlin [17]	83.457	123.157	–	136.780	–	173.724
	Present	86.147	127.498	135.545^{S}	141.927	146.727^{S}	169.047
60	Mindlin [17]	56.594	77.357	–	103.806	105.145	–
	Present	58.115	79.526	92.870^{S}	107.259	108.349	114.749^{S}
120	Mindlin [17]	49.788	54.674	63.253	–	74.838	88.418
	Present	51.147	56.107	64.865	73.149^{S}	76.759	90.769

Note: the superscript S on the data means the symmetric modes in the plate thickness direction.

to the stress concentration at the re-entrant corner, as discussed by Leissa et al. [24,25]. However, by increasing the number of terms of the admissible functions, convergence can be still rapidly achieved in the present analysis.

Table 4 gives a comparative study between the present solutions and the solutions from Liew et al. [28] where a combination of 1-D and 2-D orthogonal polynomials was used as admissible functions. It is seen for Table 4 that the present Chebyshev solutions are in good agreement with the orthogonal polynomial solutions.

Table 8
Frequency parameter $\lambda = \omega R_1^2\sqrt{\rho h/D}$ for annular sector plates with four clamped edges

h/R	θ_0	λ_1	λ_2	λ_3	λ_4	λ_5	λ_6
$R_0/R_1 = 0.25$							
0.25	120°	32.649^{AS}	44.109^{AA}	59.368^{AS}	66.765^{AS}	62.677^{SA}	75.869^{AA}
	180°	29.892^{AS}	34.712^{AA}	42.710^{AS}	52.613^{AA}	54.975^{SA}	63.388^{AS}
	240°	29.132^{AS}	31.505^{AA}	35.889^{AS}	42.012^{AA}	49.287^{AS}	52.175^{SA}
	360°	28.699^{AS}	29.553^{AA}	31.189^{AS}	33.731^{AA}	37.155^{AS}	41.320^{AA}
0.5	120°	21.365^{AS}	28.096^{AA}	31.375^{SA}	36.587^{AS}	39.410^{AS}	40.265^{SS}
	180°	19.534^{AS}	22.793^{AA}	27.509^{SA}	27.620^{AS}	33.249^{AA}	34.241^{SS}
	240°	18.959^{AS}	20.724^{AA}	23.631^{AS}	26.101^{SA}	27.362^{AA}	30.453^{SS}
	360°	18.609^{AS}	19.301^{AA}	20.536^{AS}	22.310^{AA}	24.538^{AS}	25.093^{SA}
1.0	120°	12.004^{AS}	15.551^{AA}	15.684^{SA}	19.585^{AA}	20.056^{AS}	20.099^{SS}
	180°	10.993^{AS}	12.877^{AA}	13.755^{SA}	15.514^{AS}	16.987^{SS}	17.826^{AA}
	240°	10.638^{AS}	11.745^{AA}	13.052^{SA}	13.418^{AS}	15.172^{SS}	15.450^{AA}
	360°	10.401^{AS}	10.881^{AA}	11.673^{AS}	12.548^{SA}	12.734^{AA}	13.603^{SS}
$R_0/R_1 = 0.5$							
0.25	120°	66.933^{AS}	73.194^{AA}	84.689^{AS}	101.04^{AA}	116.99^{SA}	121.05^{AS}
	180°	65.782^{AS}	68.097^{AA}	72.425^{AS}	79.084^{AA}	88.103^{AS}	99.239^{AA}
	240°	65.444^{AS}	66.619^{AA}	68.763^{AS}	72.068^{AA}	76.678^{AS}	82.641^{AA}
	360°	65.227^{AS}	65.700^{AA}	66.530^{AS}	67.770^{AA}	69.483^{AS}	71.727^{AA}
0.5	120°	43.596^{AS}	47.972^{AA}	55.488^{AS}	58.525^{SA}	65.466^{AA}	72.982^{SS}
	180°	42.748^{AS}	44.412^{AA}	47.496^{AS}	52.059^{AA}	55.181^{SA}	57.929^{AS}
	240°	42.503^{AS}	43.337^{AA}	44.887^{AS}	47.266^{AA}	50.498^{AS}	53.976^{SA}
	360°	42.352^{AS}	42.677^{AA}	43.264^{AS}	44.161^{AA}	45.410^{AS}	47.041^{AA}
1.0	120°	24.421^{AS}	27.129^{AA}	29.261^{SA}	31.468^{AS}	36.178^{SS}	36.806^{AA}
	180°	23.842^{AS}	24.982^{AA}	26.959^{AS}	27.589^{SA}	29.699^{AA}	31.211^{SS}
	240°	23.665^{AS}	24.258^{AA}	25.321^{AS}	26.870^{AA}	26.986^{SA}	28.864^{AS}
	360°	23.556^{AS}	23.789^{AA}	24.210^{AS}	24.845^{AA}	25.703^{AS}	26.552^{SA}

Note: the first superscript on the data describes the modes in the thickness direction and the second one describes those in the circumferential direction, in which A = antisymmetric mode and S = symmetric mode.

A comparative study of the present solutions with those using the three-dimensional (3-D) hierarchical finite element method is given in Table 5. It is seen from Table 5 that the present solutions are the same as those from the hierarchical finite element solutions.

It should be noted that no previously published results are known to exist for the 3-D vibration of sector plates with a re-entrant corner ($\theta > 180°$). However, Leissa et al. [24,25] provided the exact results for sector plates with a re-entrant corner, based on the Mindlin plate theory. The comparative studies of the fundamental frequency parameters are given in Table 6. It is seen from Table 6 that for thin plates ($h/R = 0.01$), there is an excellent agreement between the present 3-D solutions and the classical solutions. For moderately thick plates ($h/R = 0.2$), the present 3-D solutions also agree quite well with the Mindlin solutions. For very thick plates ($h/R = 0.4$), the discrepancies increase, particularly for C–C plates. Therefore, we can conclude that the error of the Mindlin plate theory increases with the increase of the plate thickness, particularly for very thick plates. It is well known that the Mindlin theory considers the first-order shear deformation of the plate; however, it ignores the effect of the higher-order shear deformation. It is seen from Table 6 that the maximum differences between the 3-D solutions and the Mindlin solutions always occur at the C–C plates. It has been known that the accuracy of the Mindlin solutions is dependent on the boundary conditions of the plates [31]. For a clamped edge, the rigid boundary constraints result in a rapid change of stresses and strains in the boundary layer zone, which cannot be adequately modeled by the simple constant shear Mindlin theory. In fact, Dauge and Yosibash [32] demonstrated that the Mindlin model cannot capture

Table 9
Frequency parameter $\lambda = \omega R_1^2\sqrt{\rho h/D}$ for annular sector plates with clamped straight edges and free on other edges

h/R	θ_0 (deg)	λ_1	λ_2	λ_3	λ_4	λ_5	λ_6
$R_0/R_1 = 0.25$							
0.25	120	7.4547^{AS}	16.806^{AA}	26.472^{AS}	29.111^{AS}	29.591^{SA}	34.082^{SS}
	180	3.7636^{AS}	8.3825^{AA}	14.954^{AS}	16.680^{SA}	18.451^{AS}	22.857^{AA}
	240	2.3596^{AS}	4.8540^{AA}	9.0256^{AS}	9.9743^{SA}	14.121^{AA}	14.475^{AS}
	360	1.3330^{AS}	2.0923^{AA}	4.0524^{AS}	4.2271^{SA}	6.6585^{AA}	9.2704^{SS}
0.5	120	6.3698^{AS}	12.677^{AA}	14.827^{SA}	17.098^{SS}	17.827^{AS}	20.359^{AS}
	180	3.4333^{AS}	6.9920^{AA}	8.3547^{SA}	11.787^{AS}	13.030^{SS}	13.068^{AS}
	240	2.1623^{AS}	4.2779^{AA}	4.9990^{SA}	7.6058^{AS}	9.5340^{SS}	10.771^{AS}
	360	1.1575^{AS}	1.9294^{AA}	2.2122^{SA}	3.6420^{AS}	4.6439^{SS}	5.8045^{AA}
1.0	120	4.5612^{AS}	7.4381^{SA}	7.6917^{AA}	8.5605^{SS}	9.6644^{AS}	11.360^{SA}
	180	2.7279^{AS}	4.1900^{SA}	4.7179^{AA}	6.5453^{SS}	7.3464^{AS}	7.8051^{AS}
	240	1.7701^{AS}	2.5085^{SA}	3.1603^{AA}	4.7893^{SS}	5.1971^{AS}	6.6529^{AS}
	360	0.8930^{AS}	1.0689^{SA}	1.5925^{AA}	2.3312^{SS}	2.7722^{AS}	4.0647^{SA}
$R_0/R_1 = 0.5$							
0.25	120	6.8172^{AS}	17.491^{AA}	23.455^{AS}	32.195^{AS}	36.895^{SS}	37.245^{SA}
	180	3.0170^{AS}	7.8534^{AA}	15.088^{AS}	16.519^{AS}	18.481^{SA}	24.392^{AA}
	240	1.7106^{AS}	4.1831^{AA}	8.5374^{AS}	9.9570^{SA}	13.358^{AS}	14.175^{AA}
	360	0.8566^{AS}	1.5961^{SA}	3.3885^{AS}	3.4609^{AA}	6.0005^{SA}	8.5378^{SS}
0.5	120	6.2478^{AS}	14.689^{AA}	17.813^{AS}	18.492^{SS}	18.649^{SA}	25.304^{AS}
	180	2.8772^{AS}	7.1130^{AA}	9.2573^{SA}	12.886^{AS}	13.427^{AS}	13.901^{SS}
	240	1.6295^{AS}	3.9242^{AA}	4.9899^{SA}	7.7470^{AS}	9.8354^{SS}	11.124^{AS}
	360	0.7799^{AS}	1.5309^{SA}	1.7348^{AA}	3.2025^{AS}	4.2760^{SS}	5.5690^{SA}
1.0	120	4.9679^{AS}	9.2870^{SS}	9.3518^{SA}	9.9605^{AA}	10.695^{AS}	15.215^{SA}
	180	2.5118^{AS}	4.6445^{SA}	5.4566^{AA}	6.9694^{SS}	8.4447^{AS}	9.4125^{AS}
	240	1.4453^{AS}	2.5059^{SA}	3.2636^{AA}	4.9287^{SS}	5.9447^{AS}	7.5959^{AS}
	360	0.6416^{AS}	0.8720^{AA}	1.3653^{SA}	2.1457^{SS}	2.7108^{AS}	4.0412^{AA}

See the legend of Table 8.

the boundary layer term for the clamped edge, whereas the higher-order shear deformation theories can do a much better job.

Table 7 gives a comparison of the present 3-D elasticity solutions and the 2-D Mindlin solutions for thick sector plates with four fixed edges. The radius ratio and the thickness ratio of the plates are $R_0/R_1 = 0.5$ and $h/R = 0.4$, respectively. Three different sector angles $\theta_0 = 30^\circ, 60^\circ, 120^\circ$ are considered. It is seen from Table 7 that the Mindlin solutions are always lower than the present 3-D elasticity solutions. Moreover, it is seen that the Mindlin solutions cannot give the extending modes (i.e. the symmetric modes in the plate thickness direction), which could go into the low-order modes of the thick plates. However, the present 3-D analysis can provide a complete vibration spectrum that is composed of antisymmetric modes and symmetric modes in the plate thickness direction.

4. Numerical results

In this section, some benchmark results are presented in Tables 8–11 for comparisons with results from other methods. Four boundary conditions are considered: four clamped edges, two clamped straight edges and the other edges free, four hard simply supported edges, two straight edges free and the other edges clamped. Considering the symmetry of the boundary conditions in the θ direction, the vibration modes can be divided into four cases: antisymmetric in the z direction and antisymmetric in the θ direction (AA mode), antisymmetric in the z direction and symmetric in the θ direction (AS mode), symmetric in the z direction and

Table 10
Frequency parameter $\lambda = \omega R_1^2\sqrt{\rho h/D}$ for annular sector plates with four edges simply supported

h/R	θ_0 (deg)	λ_1	λ_2	λ_3	λ_4	λ_5	λ_6
$R_0/R_1 = 0.25$							
0.25	120	21.069^{AS}	26.194^{SS}	33.633^{AA}	39.806^{SA}	48.611^{SA}	50.145^{AS}
	180	18.561^{AS}	24.532^{AA}	26.192^{SS}	29.223^{SA}	33.633^{AS}	39.806^{SS}
	240	17.690^{AS}	21.069^{AA}	26.194^{SA}	26.573^{AS}	27.402^{SS}	31.505^{SS}
	360	17.075^{AS}	18.561^{AA}	21.069^{AS}	24.532^{AA}	26.192^{SA}	26.194^{SS}
0.5	120	13.115^{SS}	16.462^{AS}	19.911^{SA}	24.306^{SA}	24.635^{AA}	29.027^{SS}
	180	13.119^{SS}	14.625^{SA}	14.650^{AS}	18.836^{AA}	19.911^{SS}	24.306^{SA}
	240	13.115^{SA}	13.725^{SS}	13.996^{AS}	15.763^{SS}	16.462^{AA}	19.911^{SA}
	360	13.115^{SS}	13.119^{SA}	13.515^{AS}	14.588^{SS}	14.625^{SA}	14.650^{AA}
1.0	120	6.5742^{SS}	9.9622^{SA}	10.513^{AS}	12.153^{SA}	13.326^{AS}	14.518^{SS}
	180	6.5803^{SS}	7.3240^{SA}	9.4280^{AS}	9.9622^{SS}	11.840^{AA}	12.153^{SA}
	240	6.5742^{SA}	6.8824^{SS}	7.8915^{SS}	9.0126^{AS}	9.9622^{SA}	10.513^{AA}
	360	6.5743^{SS}	6.5804^{SA}	7.3092^{SS}	7.3240^{SA}	8.5374^{SS}	8.7024^{AS}
$R_0/R_1 = 0.5$							
0.25	120	39.493^{AS}	44.178^{SS}	49.082^{AA}	63.496^{SA}	64.190^{AS}	83.553^{AA}
	180	37.681^{AS}	40.107^{SS}	42.013^{AA}	49.082^{AS}	49.618^{SA}	58.614^{AA}
	240	37.044^{AS}	38.652^{SS}	39.493^{AA}	43.532^{AS}	44.178^{SA}	49.082^{AA}
	360	36.589^{AS}	37.607^{SS}	37.681^{AA}	39.493^{AS}	40.107^{SA}	42.013^{AA}
0.5	120	22.119^{SS}	31.762^{SA}	31.853^{AS}	38.449^{AA}	44.135^{SS}	48.273^{AS}
	180	20.090^{SS}	24.833^{SA}	30.567^{AS}	31.762^{SS}	33.620^{AA}	38.449^{AS}
	240	19.366^{SS}	22.119^{SA}	26.404^{SS}	30.112^{AS}	31.762^{SA}	31.853^{AA}
	360	18.846^{SS}	20.090^{SA}	22.119^{SS}	24.833^{SA}	28.094^{SS}	29.785^{AS}
1.0	120	11.090^{SS}	15.894^{SA}	20.984^{AS}	22.074^{SS}	24.682^{AA}	26.204^{SA}
	180	10.083^{SS}	12.439^{SA}	15.894^{SS}	19.940^{SA}	20.232^{AS}	21.997^{AA}
	240	9.7248^{SS}	11.090^{SA}	13.222^{SS}	15.894^{SA}	18.894^{SS}	19.964^{AS}
	360	9.4674^{SS}	10.083^{SA}	11.090^{SS}	12.439^{SA}	14.064^{SS}	15.894^{SA}

See the legend of Table 8.

antisymmetric in the θ direction (SA mode), symmetric in the z direction and symmetric in the θ direction (SS mode). It can be seen from Tables 7 to 10 that with the increase of the thickness ratio, the symmetric mode in the thickness direction falls into the scope of the low-order frequencies, which cannot be obtained from the classical plate or Mindlin plate theories. For example, when $h/R = 0.5$ and $h/R = 1.0$, the fundamental frequency of the simply supported plates is symmetric mode in the thickness direction. It is well known that the 2-D theories, either the thin plate theory or the Mindlin theory, cannot predict the symmetric mode in the thickness direction. The ability to find the symmetric mode in the thickness direction is an important contribution of the 3-D elasticity analysis. It is seen from Tables 8 to 11 that the frequency parameters monotonically decrease with the increase of the sector angle and the plate thickness; however, they monotonically increase with the increase of the radius ratio.

In the 2-D plate theories, the simply supported edge means zero transverse displacement at the edge and zero moment along the edge. However, in the 3-D analysis, there are two kinds of simply supported definitions. One is the zero transverse displacement (the displacement in the z direction) at the edge and the zero tangential displacement along the edge, which is called hard simply supported. The other case requires only zero transverse displacement at the edge, which is called soft simply supported. Two kinds of simple supports correspond to different boundary functions as shown in Table 1. Table 12 gives a comparison of frequency parameters between two kinds of simple supports. It is shown from Table 12 that for thin plates ($h/R = 0.01$), the frequency difference between hard simple supports and soft simple supports is negligible. However, with the increase of plate thickness, the frequency difference between the two kinds of simple

Table 11
Frequency parameter $\lambda = \omega R_1^2\sqrt{\rho h/D}$ for annular sector plates with free straight edges and the other edges clamped

h/R	θ_0 (deg)	λ_1	λ_2	λ_3	λ_4	λ_5	λ_6
$R_0/R_1 = 0.25$							
0.25	120	28.181^{AS}	29.502^{AA}	35.816^{AS}	45.545^{SA}	48.301^{AA}	56.486^{SS}
	180	28.255^{AS}	28.803^{AA}	31.455^{AS}	37.009^{AA}	45.465^{AS}	46.476^{SA}
	240	28.292^{AS}	28.570^{AA}	30.009^{AS}	32.926^{AA}	37.679^{AS}	44.061^{AA}
	360	28.327^{AS}	28.424^{AA}	29.051^{AS}	30.202^{AA}	32.088^{AS}	34.822^{AA}
0.5	120	18.278^{AS}	19.210^{AA}	22.789^{SA}	23.488^{AS}	28.268^{SS}	30.955^{AA}
	180	18.309^{AS}	18.748^{AA}	20.628^{AS}	23.250^{SA}	24.364^{AA}	25.553^{SS}
	240	18.326^{AS}	18.571^{AA}	19.623^{AS}	21.703^{AA}	23.459^{SA}	24.607^{SS}
	360	18.344^{AS}	18.445^{AA}	18.915^{AS}	19.788^{AA}	21.168^{AS}	23.068^{AA}
1.0	120	10.196^{AS}	10.763^{AA}	11.408^{SA}	13.310^{AS}	14.062^{SS}	15.673^{AA}
	180	10.206^{AS}	10.517^{AA}	11.634^{SA}	11.700^{AS}	12.770^{SS}	13.687^{AA}
	240	10.213^{AS}	10.400^{AA}	11.092^{AS}	11.736^{SA}	12.308^{SS}	12.350^{AA}
	360	10.221^{AS}	10.306^{AA}	10.632^{AS}	11.215^{AA}	11.829^{SA}	12.017^{SS}
$R_0/R_1 = 0.5$							
0.25	120	64.789^{AS}	65.627^{AA}	69.384^{AS}	76.942^{AA}	89.353^{AS}	101.43^{SA}
	180	64.860^{AS}	65.190^{AA}	66.846^{AS}	69.897^{AA}	74.814^{AS}	81.933^{AA}
	240	64.896^{AS}	65.055^{AA}	66.004^{AS}	67.633^{AA}	70.174^{AS}	73.814^{AA}
	360	64.927^{AS}	64.975^{AA}	65.435^{AS}	66.124^{AA}	67.155^{AS}	68.581^{AA}
0.5	120	42.118^{AS}	42.639^{AA}	45.052^{AS}	50.303^{AA}	50.739^{SA}	55.538^{SS}
	180	42.151^{AS}	42.371^{AA}	43.412^{AS}	45.498^{AA}	48.983^{AS}	51.187^{SA}
	240	42.168^{AS}	42.281^{AA}	42.869^{AS}	43.962^{AA}	45.747^{AS}	48.355^{AA}
	360	42.185^{AS}	42.225^{AA}	42.498^{AS}	42.952^{AA}	43.655^{AS}	44.660^{AA}
1.0	120	23.431^{AS}	23.745^{AA}	25.304^{AS}	25.383^{SA}	27.744^{SS}	28.540^{AA}
	180	23.443^{AS}	23.590^{AA}	24.255^{AS}	25.603^{SA}	25.658^{AA}	26.527^{SS}
	240	23.450^{AS}	23.532^{AA}	23.905^{AS}	24.648^{AA}	25.706^{SA}	25.868^{AS}
	360	23.458^{AS}	23.491^{AA}	23.661^{AS}	23.969^{AA}	24.459^{AS}	25.163^{AA}

See the legend of Table 8.

supports increases, particularly for plates with large sector angles. The effect of simple support conditions is important on the low-order frequencies, particularly on the fundamental frequency. For example, for plate with $h/R = 0.4$ and $\theta = 270^\circ$ the fundamental frequency parameters corresponding to hard and soft simple supports are 23.942 versus 3.1029. Therefore, for thick sector plates the simple supported boundaries should be carefully defined.

The present method can be extended to study the 3-D vibration of shallow helicoidal shells with a small helix angle [25]. Table 13 gives the first six frequency parameters of thin helicoidal shells for $\theta = 390$–480° with an incremental angle 30°. It should be noted that the present solutions are only suitable for the approximate estimations of low-order eigenfrequencies of the helicoidal shells with very small helix angle.

Figs. 2–4 give the vibration modes of thick sector plates with clamped straight edges and free on other edges. The sector angle and the radius ratio are, respectively, $\theta = 120^\circ$ and $R_0/R_1 = 0.5$. The first six modes for three different thickness ratios $h/R = 0.25$, 0.5 and 1.0 are presented. It is seen from Figs. 2 to 4 that the antisymmetric modes in the thickness direction exhibit the flexural vibrations while the symmetric modes in the thickness direction exhibit the extending vibrations. With an increase of plate thickness, the symmetric modes in the thickness direction move down in the list of low-order eigenfrequencies. When $h/R = 0.25$, the fifth and sixth frequencies are those of the symmetric modes in the thickness direction. When $h/R = 0.5$, the fourth and fifth frequencies are those of the symmetric modes in the thickness direction. When $h/R = 1.0$, the second, third and sixth frequencies are those of the symmetric modes in the thickness direction.

Table 12
Comparison of frequency parameter $\lambda = \omega R_1^2\sqrt{\rho h/D}$ for annular sector plates with (a) four hard simply-supported edges and (b) four soft simply supported edges, $R_0/R_1 = 0.5$

θ_0 (deg)	BC	λ_1	λ_2	λ_3	λ_4	λ_5	λ_6
$h/R = 0.01$							
90	Hard	47.079^{AS}	68.359^{AA}	103.39^{AS}	150.88^{AA}	166.22^{AS}	189.44^{AA}
	Soft	46.997^{AS}	68.150^{AA}	103.11^{AS}	150.56^{AA}	166.13^{AS}	189.10^{AA}
180	Hard	41.790^{AS}	47.079^{AA}	55.943^{AS}	68.359^{AA}	84.226^{AS}	103.39^{AA}
	Soft	41.771^{AS}	47.013^{AA}	55.823^{AS}	68.192^{AA}	84.028^{AS}	103.17^{AA}
270	Hard	40.815^{AS}	43.158^{AA}	47.079^{AS}	52.591^{AA}	59.690^{AS}	68.359^{AA}
	Soft	40.807^{AS}	43.129^{AA}	47.020^{AS}	52.500^{AA}	59.569^{AS}	68.211^{AA}
$h/R = 0.2$							
90	Hard	43.609^{AS}	61.536^{AA}	62.011^{SS}	89.094^{AS}	99.631^{SA}	123.33^{AA}
	Soft	42.320^{AS}	58.512^{AA}	51.925^{SS}	85.528^{AS}	88.642^{SS}	98.788^{SA}
180	Hard	38.992^{AS}	43.609^{AA}	50.115^{SS}	51.198^{AS}	61.536^{AA}	62.011^{SA}
	Soft	14.323^{SS}	35.273^{SA}	38.650^{AS}	42.443^{AA}	49.142^{AS}	56.170^{SS}
270	Hard	38.133^{AS}	40.192^{AA}	43.609^{AS}	47.802^{SS}	48.349^{AA}	53.305^{SA}
	Soft	6.1718^{SS}	15.271^{SA}	30.057^{SS}	37.982^{AS}	39.630^{AA}	42.485^{AS}
$h/R = 0.4$							
90	Hard	31.030^{SS}	36.875^{AS}	49.825^{SA}	49.862^{AA}	65.510^{SA}	68.350^{AS}
	Soft	26.087^{SS}	35.402^{AS}	44.367^{SS}	46.897^{AA}	49.539^{SA}	65.311^{AS}
180	Hard	25.095^{SS}	31.030^{SA}	33.365^{AS}	36.875^{AA}	39.694^{SS}	42.487^{AS}
	Soft	7.1998^{SS}	17.717^{SA}	28.146^{SS}	32.220^{SS}	32.938^{AS}	35.491^{AA}
270	Hard	23.942^{SS}	26.685^{SA}	31.030^{SS}	32.704^{AS}	34.285^{AA}	36.590^{SA}
	Soft	3.1029^{SS}	7.6741^{SA}	15.096^{SS}	23.824^{SA}	25.706^{SS}	32.510^{AS}

Table 13
Frequency parameter $\lambda = \omega R_1^2\sqrt{\rho h/D}$ for shallow helicoidal shells with $h/R = 0.01$

R_0/R_1	θ_0 (deg)	λ_1	λ_2	λ_3	λ_4	λ_5	λ_6
Shallow helicoidal shells with four free edges							
0.25	390	1.358^{AA}	2.768^{AS}	5.454^{AA}	5.702^{AS}	9.616^{AS}	9.792^{AA}
	420	1.157^{AA}	2.287^{AS}	4.593^{AA}	6.278^{AS}	8.630^{AS}	9.015^{AA}
	450	1.027^{AA}	1.895^{AS}	3.877^{AA}	5.728^{AS}	8.010^{AS}	8.218^{AA}
	480	0.9500^{AA}	1.582^{AS}	3.278^{AA}	5.110^{AS}	7.406^{AA}	7.624^{AS}
0.5	390	0.8963^{AA}	2.145^{AS}	4.392^{AA}	6.666^{AS}	9.168^{AA}	9.398^{AS}
	420	0.7485^{AA}	1.728^{AS}	3.628^{AA}	5.830^{AS}	8.273^{AA}	8.838^{AS}
	450	0.6538^{AA}	1.403^{AS}	3.007^{AA}	5.027^{AS}	7.349^{AA}	8.429^{AS}
	480	0.5960^{AA}	1.150^{AS}	2.500^{AA}	4.315^{AS}	6.460^{AA}	8.002^{AS}
Shallow helicoidal shells with clamped straight edges and the other edges free							
0.25	390	1.356^{AS}	1.854^{AA}	3.591^{AS}	6.038^{AA}	9.055^{AS}	12.60^{AA}
	420	1.257^{AS}	1.609^{AA}	3.040^{AS}	5.140^{AA}	7.779^{AS}	10.87^{AA}
	450	1.172^{AS}	1.428^{AA}	2.601^{AS}	4.406^{AA}	6.730^{AS}	9.463^{AA}
	480	1.098^{AS}	1.295^{AA}	2.248^{AS}	3.800^{AA}	5.856^{AS}	8.287^{AA}
0.5	390	0.8232^{AS}	1.352^{AA}	2.853^{AS}	5.163^{AA}	8.136^{AS}	11.69^{AA}
	420	0.7520^{AS}	1.147^{AA}	2.354^{AS}	4.310^{AA}	6.869^{AS}	9.951^{AA}
	450	0.6954^{AS}	0.9991^{AA}	1.961^{AS}	3.625^{AA}	5.842^{AS}	8.534^{AA}
	480	0.6494^{AS}	0.8893^{AA}	1.650^{AS}	3.069^{AA}	4.999^{AS}	7.366^{AA}

See the legend of Table 8.

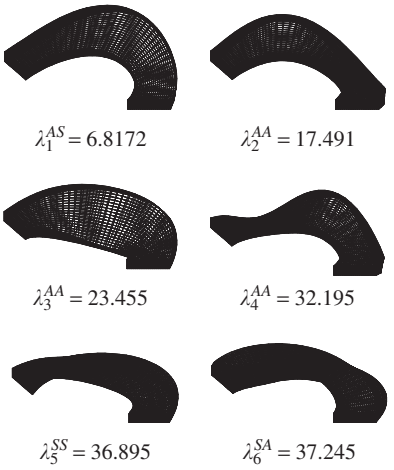

Fig. 2. The first six modes of the sector plate with clamped straight edges and free on other edges, $R_0/R_1 = 0.5$, $h/R = 0.25$, $\alpha = 120^\circ$. The first superscript on λ describes the modes in the thickness direction and the second one describes those in the circumferential direction.

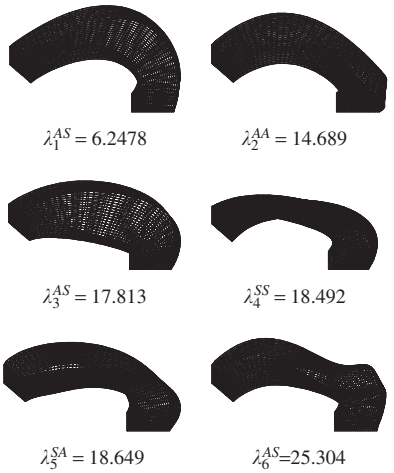

Fig. 3. The first six modes of the sector plate with clamped straight edges and free on other edges, $R_0/R_1 = 0.5$, $h/R = 0.5$, $\alpha = 120^\circ$.

5. Conclusions

The 3-D vibration analysis of thick sector plates has been presented. The analysis is based on the 3-D linear small strain elasticity theory. The Chebyshev–Ritz method expressed in terms of cylindrical coordinates is used to obtain frequency parameters of thick sector plates under various support conditions. High accuracy, rapid convergence and numerical robustness of the present method have been demonstrated. A complete set of free vibration spectrum for thick annular sector plates have been provided from the present analysis, which cannot be obtained by the CPT or the Mindlin plate theory. Some benchmark results are provided in tabulation for the first time such as the frequency parameters of plates with re-entrant sector angle and the shallow helicoidal shells. The effect of simply supported conditions on frequency parameters of thick sector plates has also been discussed in detail.

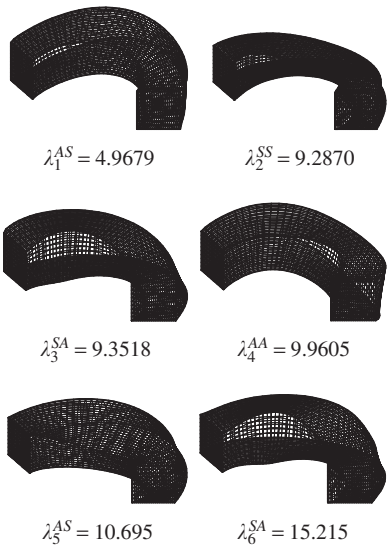

Fig. 4. The first six modes of sector plate with clamped straight edges and free on the other edges, $R_0/R_1 = 0.5$, $h/R = 1.0$, $\alpha = 120^\circ$.

References

[1] R. Ramakris, V.X. Kunukkas, Free vibration of annular sector plates, *Journal of Sound and Vibration* 30 (1973) 127–129.
[2] M. Mukhopadhyay, A semi-analytic solution for free vibration of annular sector plates, *Journal of Sound and Vibration* 63 (1979) 87–95.
[3] M. Mukhopadhyay, Free vibration of annular sector plates with edges possessing different degrees of rotational restraints, *Journal of Sound and Vibration* 80 (1982) 275–279.
[4] R.S. Srinivasan, V. Thiruvenkatachari, Free vibration of annular sector plates by an integral equation technique, *Journal of Sound and Vibration* 89 (1983) 425–432.
[5] R.S. Srinivasan, V. Thiruvenkatachari, Free vibration analysis of laminated annular sector plates, *Journal of Sound and Vibration* 109 (1986) 89–96.
[6] C.S. Kim, S.M. Dickinson, On the free, transverse vibration of annular and circular, thin, sectorial plates subjected to certain complicating effects, *Journal of Sound and Vibration* 134 (1989) 407–421.
[7] K.M. Liew, K.Y. Lam, On the use of 2-d orthogonal polynomials in the Rayleigh–Ritz method for flexural vibration of annular sector plates of arbitrary shape, *International Journal of Mechanical Sciences* 35 (1993) 129–139.
[8] K. Ramaiah, K. Vijayakumar, Natural frequencies of circumferentially truncated sector plates with simply supported straight edges, *Journal of Sound and Vibration* 34 (1974) 53–61.
[9] T. Irie, K. Tanaka, G. Yamada, Free vibration of a cantilever annular sector plate with curved radial edges, *Journal of Sound and Vibration* 122 (1988) 69–78.
[10] T. Mizusawa, Application of the spline element method to analyze vibration of annular sector plates, *Journal of Sound and Vibration* 149 (1991) 461.
[11] T. Mizusawa, T. Kajita, Vibration of annular plates using spline strip method, *Communications in Applied Numerical Methods* 8 (1992) 537–546.
[12] M. Swaminadham, J. Danielski, O. Mahrenholtz, Free vibration analysis of annular sector plates by holographic experiments, *Journal of Sound and Vibration* 95 (1984) 333–340.
[13] J.W. Seok, H.F. Tiersten, Free vibrations of annular sector cantilever plates—part 1: out-of-plane motion, *Journal of Sound and Vibration* 271 (2004) 757–772.
[14] A. Houmat, Asector Fourier p-element applied to free vibration analysis of sectorial plates, *Journal of Sound and Vibration* 243 (2001) 269–282.
[15] A. Sharma, H.B. Sharda, Y. Nath, Stability and vibration of Mindlin sector plates: an analytical approach, *AIAA Journal* 43 (2005) 1109–1116.
[16] A. Sharma, H.B. Sharda, Y. Nath, Stability and vibration of thick laminated composite sector plates, *Journal of Sound and Vibration* 287 (2005) 1–23.
[17] K.M. Liew, F.L. Liu, Differential quadrature method for vibration analysis of shear deformable annular sector plates, *Journal of Sound and Vibration* 230 (2000) 335–356.
[18] M.N. Bapu Rao, P. Guruswamy, K.S. Sampath Kumaran, Finite element analysis of thick annular and sector plates, *Nuclear Engineering and Design* 62 (1979) 505–516.

[19] P. Guruswamy, T.Y. Yang, A sector finite element for dynamic analysis of thick plates, *Journal of Sound and Vibration* 62 (1979) 505.
[20] P.R. Benson, E. Hinton, A thick finite strip solution for static, free vibration and stability problems, *International Journal for Numerical Methods in Engineering* 10 (1976) 665–678.
[21] M.S. Cheung, M.Y.T. Chan, Static and dynamic analysis of thin and thick sectorial plates by the finite strip method, *Computers and Structures* 14 (1981) 79–88.
[22] T. Mizusawa, Vibration of thick annular sector plates using semi-analytical methods, *Journal of Sound and Vibration* 150 (1991) 245.
[23] Y. Xiang, K.M. Liew, S. Kitipornchai, Transverse vibration of thick annular sector plates, *Journal of Engineering Mechanics—ASCE* 119 (1993) 1579–1599.
[24] A.W. Leissa, O.G. McGee, C.S. Huang, Vibrations of sectorial plates having corner stress singularities, *Journal of Applied Mechanics—Transactions of the ASME* 60 (1993) 134–140.
[25] O.G. McGee, C.S. Huang, A.W. Leissa, Comprehensive exact solutions for free vibrations of thick annular sectorial plates with simply supported radial edges, *International Journal of Mechanical Sciences* 37 (1995) 537–566.
[26] T. Mizusawa, Vibration of thick annular sector plates using semi-analytical methods, *Journal of Sound and Vibration* 150 (1991) 245–259.
[27] A. Houmat, Three-dimensional hierarchical finite element free vibration analysis of annular sector plates, *Journal of Sound and Vibration* 276 (2004) 181–193.
[28] K.M. Liew, T.Y. Ng, B.P. Wang, Vibration of annular sector plates from three-dimensional analysis, *Journal of the Acoustical Society of America* 110 (2001) 233–242.
[29] L. Fox, I.B. Parker, *Chebyshev Polynomials in Numerical Analysis*, Oxford University Press, London, 1968.
[30] D. Zhou, Three-dimensional Vibration Analysis of Structural Elements Using Chebyshev–Ritz Method, PhD Thesis, The University of Hong Kong, 2003.
[31] M. Dauge, Z. Yosibash, Eigen-frequencies in thin elastic 3-D domains and Reissner–Mindlin plate models, *Mathematical Methods in the Applied Sciences* 25 (2002) 21–48.
[32] M. Dauge, Z. Yosibash, Boundary layer realization in thin elastic three dimensional domains and two-dimensional hierarchic plate models, *International Journal of Solids and Structures* 37 (2000) 2443–2471.